CHAPTER VI
HYDROGEN STORAGE BEHAVIORS OF $LiBH_4/MgH_2$: EFFECTS OF TITANIUM CATALYSTS

6.1 Abstract

A 2:1 molar ratio of $LiBH_4/MgH_2$ doped with 3 mol% of a titanium catalyst (Ti, TiO_2, and $TiCl_3$) was studied for its hydrogen desorption/absorption properties. The results in the first desorption showed that the sample doped with $TiCl_3$ was more active than the other samples as it released hydrogen in one step, while there were three steps for the other samples. However, all samples started to desorb hydrogen at the same temperature of 50°C. The undoped sample had the highest amount of hydrogen (9.2 wt%). In the subsequent desorption, all samples decomposed in two steps, and the one doped with $TiCl_3$ had the lowest desorption temperature, followed by TiO_2-$2LiBH_4$+MgH_2, $2LiBH_4$+MgH_2, and Ti-$2LiBH_4$+MgH_2. Using Ti resulted in the highest amount of hydrogen at 5.0 wt%. A possible reason could be the formation of titanium hydride during the hydrogen desorption. However, the titanium hydride formation depended on the composition and the chemical state of titanium catalyst. $TiH_{1.971}$ and $TiH_{0.71}$ were formed from the doping of Ti and the doping of TiO_2 and $TiCl_3$, respectively.

6.2 Introduction

Hydrogen storage for transportation must meet weight, cost, life time, and safety requirements. As compared with traditional storage methods such as in a high pressure gas tank and in the liquefied form, storing hydrogen in solid state hydride materials has more potential in terms of gravimetric and volumetric hydrogen density and reversibility property [1]. However, their thermodynamics and kinetics are too stable for practical mobile applications [2-4]. Examples of these materials are $NaAlH_4$, $LiAlH_4$, MgH_2, and $LiBH_4$. For $NaAlH_4$, it contains totally 5.6 wt% hydrogen, which is slightly lower than the DOE's target at 6.0 wt% in 2010.

However, efforts have been dedicated to $NaAlH_4$, in part, because it offers a reasonable decomposition temperature, 120°C [5,6]. $LiAlH_4$ has a high hydrogen capacity of 10.5 wt% but only 5.3 wt% hydrogen can be released at 150°C. However, its hydrogen desorption/absorption is irreversible [7]. MgH_2 is widely studied because it is abundance and the total amount of hydrogen is quite high (7.6 wt%). However, the decomposition takes place at a temperature higher than 350°C and its reaction kinetics is very slow [8,9].

In the case of $LiBH_4$, it is one of the most attractive materials because it provides high hydrogen capacity of 18.4 wt%. On the other hand, the hydrogen desorption starts at a temperature higher than 400°C and the reaction is difficult to reverse [10]. However, an addition of a suitable catalyst can improve the hydrogen desorption/absorption properties of $LiBH_4$ [11-13]. In 2003, Züttel et al. [14,15] succeeded in reduce the decomposition temperature of $LiBH_4$ by doping with 75 wt% SiO_2. The results showed that the hydrogen desorption started at 200°C and decomposed the total hydrogen of 9 wt%. Au et al. [16-18] reduced the hydrogen desorption temperature and improved the reversibility of $LiBH_4$ by adding various types of metal oxide and metal chloride catalysts. For the use of metal oxide catalysts, they found that the addition of 25 wt% TiO_2 could desorb 9.0 wt% hydrogen in a temperature range from 100 to 600°C and absorb 8.0 wt% hydrogen at 600°C and 7.0 MPa hydrogen. However, the reversible hydrogen storage capacity of $LiBH_4$ gradually decreased due to the loss of boron during the hydrogen desorption. In the case of metal chloride catalysts, 1-2 mol% of $MgCl_2$ and $TiCl_3$ were added into $LiBH_4$. The sample released 5.0 wt% hydrogen in a temperature range from 60 to 450°C and absorbed 4.5 wt% hydrogen at 600°C and 7.0 MPa hydrogen.

It is well-known that alloying and/or reacting $LiBH_4$ with a metal and/or a metal hydride through ball milling, so called reactive hydride composite (RHC) [19-21], can improve the thermodynamic properties such as reaction enthalpy due to the changing of reaction partway. Vajo et al. [22], who first applied the RHC concept to $LiBH_4$, studied the mixture of LiH and MgB_2 (a 2:1 molar ratio) including 2-3 mol% $TiCl_3$. The results showed that the mixture reversibly stored about 8-10 wt% hydrogen, and the decomposition occurred in two steps at 270 and 380°C,

respectively. It was concluded that the RHC not only lowered the hydrogen desorption temperature, but also contributed the reversibility due to the formation of MgB_2 during hydrogen desorption. Fan et al. [23] studied a 1:2 mass ratio of $LiBH_4$ and MgH_2 doped with 16 wt% Nb_2O_5. It was found that the sample started to release hydrogen at 300°C and desorbed 6-8 wt% hydrogen. The hydrogen absorption of 5-6 wt% was achieved at 400°C and 1.9 MPa hydrogen.

A titanium based catalyst is one of the most effective catalysts for the solid state hydride development. For instance, Bogdanović and Schwickardi [5] studied the Pressure-Composition Isotherm of $NaAlH_4$ doped with $TiCl_3$. The results revealed the two temperature-dependent pressure plateaus corresponding to the two-step reversibly stored 4.2-3.1 and 2.7-2.1 wt% hydrogen in each step. Sandrock et al. [6] studied the behaviors of $TiCl_3$ catalyst in $NaAlH_4$. They reported that $TiCl_3$ was reduced to metallic Ti (Ti) during the ball-milling process. In addition, Ti could increase both hydrogen desorption and absorption kinetics but it reduced the hydrogen capacity of $NaAlH_4$. Chen et al. [24] doped $LiAlH_4$ and Li_3AlH_6 with $TiCl_3 + 1/3AlCl_3$ and measured the thermodynamic and the kinetic properties over a temperature range from 25 to 250°C. They found that the activation energies from the Arrhenius plot were 42.6 and 54.8 kJ $(mol\ H_2)^{-1}$ for the hydrogen desorption of $LiAlH_4$ and Li_3AlH_6, respectively. Furthermore, the defect sites of a titanium catalyst ($Ti^0/Ti^{2+}/Ti^{3+}$) played an important role in the reversibility improvement [25].

In this work, roles of titanium based catalysts including Ti-metallic (Ti), TiO_2, and $TiCl_3$ on the hydrogen desorption temperature, total hydrogen storage capacity, reversibility, and reaction kinetics of a 2:1 mole ratio of the $LiBH_4$ and MgH_2 mixture were studied. XRD characterization was conducted in order to investigate the phase transformation of the sample at different conditions and evaluate the crystallite size of hydrides.

6.3 Experimental

To prevent the sample contamination by air and moisture, all sample handling steps were performed in a glovebox filled with nitrogen gas. The starting

materials of $LiBH_4$ (95%, Acros Organics) and MgH_2 (90%, Mg 10%, Acros Organics), and titanium based catalysts, Ti (99.98%, Sigma Aldrich) and TiO_2 (Degüssa P25) were used without further purification. $TiCl_3$ was prepared by vacuum drying of 12% $TiCl_3$ solution in hydrochloric acid. The hydride sample was prepared from a 2:1:0.09 molar ratio of $LiBH_4$, MgH_2, and a titanium catalyst, and ball-milled by using a centrifugal ball mill (Retsch ball mill model S100) under nitrogen atmosphere with a ball to powder ratio of 60:1 and a rotation speed of 300 rpm for 5 h. To evaluate the hydrogen desorption/absorption properties, approximately 0.3 g of the milled sample was tested in the calibrated-Sievert's type apparatus. The hydrogen desorption was carried out under 0.1 MPa H_2 (purity 99.9999%) from 25 to 500°C with a heating rate of 2°C min^{-1}. The hydrogen absorption was performed under 8.5 MPa H_2 and 350°C for 12 h. Both hydrogen desorption and absorption were repeated in order to investigate the reversibility of the sample. The accumulated pressure released from the sample was measured by a pressure transducer (Cole Parmer, model 68073-68074), and used for calculating the hydrogen desorption capacity.

For the sample characterization, a Rigaku X-ray diffractometer (model DMAX 2200 HV) was used to identify phase transformation and determine the crystallite size of hydrides. The sample was packed on a glass plate covered by a Kapton tape to prevent air and moisture. The measurement was carried out at the room temperature over a range of diffraction angles from 20 to 80 with Cu Kα radiation (40 kV, 30 mA).

6.4 Results and Discussion

It is well-known that the performance of metal hydrides and complex metal hydrides such as $NaAlH_4$, $LiAlH_4$, MgH_2 and $LiBH_4$ are dramatically improved when a titanium catalyst was applied [5,6,26-28]. However, there are many types of titanium catalysts, each of which provides different effects on the hydrogen desorption/absorption properties of the hydride. In this work, 3 mol% of a titanium

catalyst (Ti, TiO_2, and $TiCl_3$) was added into the $2LiBH_4/MgH_2$ mixture and ball-milled for 5 h.

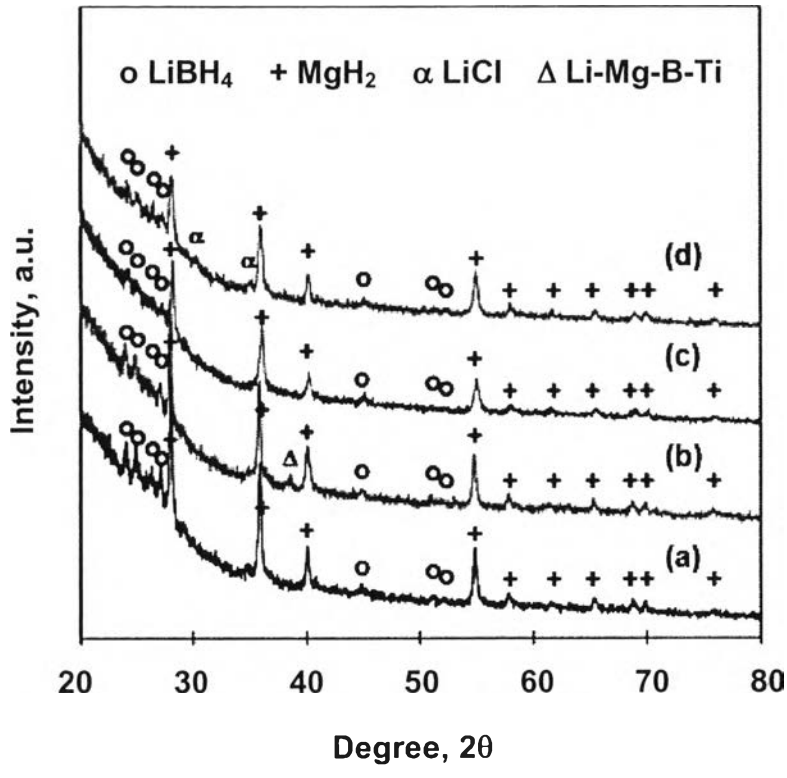

Figure 6.1 XRD patterns of the samples after ball-milling for 5 h (a) undoped, (b) Ti-, (c) TiO_2-, and (d) $TiCl_3$-$LiBH_4/MgH_2$ mixture.

The XRD patterns of the $2LiBH_4/MgH_2$ mixture after ball-milling are shown in Fig. 6.1. It can be seen that the peak intensities of all doped samples (Figs. 1(b)-(d)) are weaker and boarder than the undoped one (Fig. 6.1(a)). This implies that the titanium catalysts can reduce the crystallite size as well as increase the lattice strain of $LiBH_4$ and MgH_2. The crystallite sizes of samples can be calculated by using the Scherrer equation and shown in Table 6.1. The results confirm the reduction in the crystallite sizes of both hydrides with the titanium catalyst doping. However, the titanium catalysts seem to reduce the crystallite size of MgH_2 in a greater extent than that of $LiBH_4$. In addition, among the doped samples, the one with Ti has the largest crystallite size. A possible reason may be due to the hardness of the Ti particles, which is higher than that of TiO_2 and $TiCl_3$ particles. It was

reported that the hardness of a catalyst affects the particle size and the crystallite size reduction of a hydride [29]. In addition, the XRD patterns after ball-milling reveal that the samples doped with Ti (Fig. 6.1(b)) and $TiCl_3$ (Fig. 6.1(d)) form new phases of Li-Mg-B-Ti and LiCl, respectively. The alloy phase of Li-Mg-B-Ti may also form due to the incorporation between the defect sites of Ti^0 and the host metal lattice frameworks of $LiBH_4$ and MgH_2 during the ball-milling. In addition, the LiCl phase is produced from the reaction between Li^+ and Cl^-, which are from the partial decomposition of $LiBH_4$ and $TiCl_3$, respectively.

Table 6.1 Crystallite sizes of $LiBH_4$ and MgH_2 in the $LiBH_4/MgH_2$ mixture and the mixture doped with a titanium catalyst after ball-milling for 5 h

Titanium catalyst	$LiBH_4$, nm	MgH_2, nm
Undoped	25.57	37.24
Ti	25.31	27.71
TiO_2	24.27	24.06
$TiCl_3$	24.78	21.55

Hydrogen desorption profiles in the first to the forth desorption of the $LiBH_4/MgH_2$ mixture and the mixture doped with 3 mol% of Ti, TiO_2, and $TiCl_3$ are shown in Figs. 6.2-6.5, respectively. Details of the hydrogen desorption temperatures and the amounts of released hydrogen are in Table 6.2.

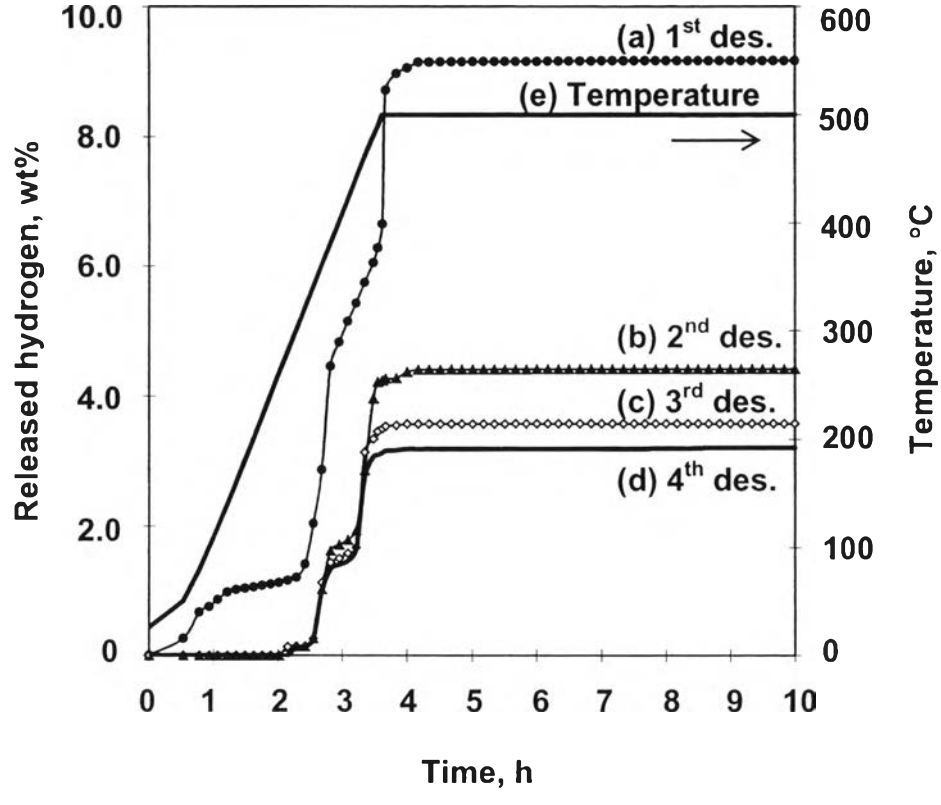

Figure 6.2 Hydrogen desorption profiles of the undoped $LiBH_4/MgH_2$ mixture after ball-milling for 5 h (a) first, (b) second, (c) third, (d) forth hydrogen desorption, and (e) temperature.

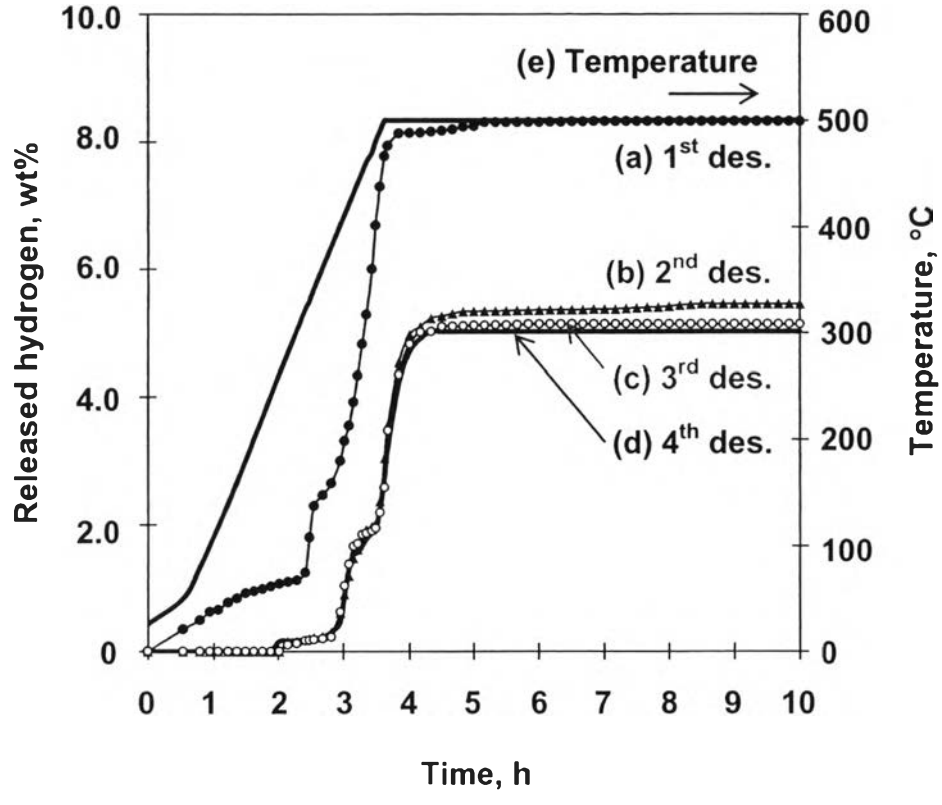

Figure 6.3 Hydrogen desorption profiles of the Ti-$LiBH_4$/MgH_2 mixture after ball-milling for 5 h (a) first, (b) second, (c) third, (d) forth hydrogen desorption, and (e) temperature.

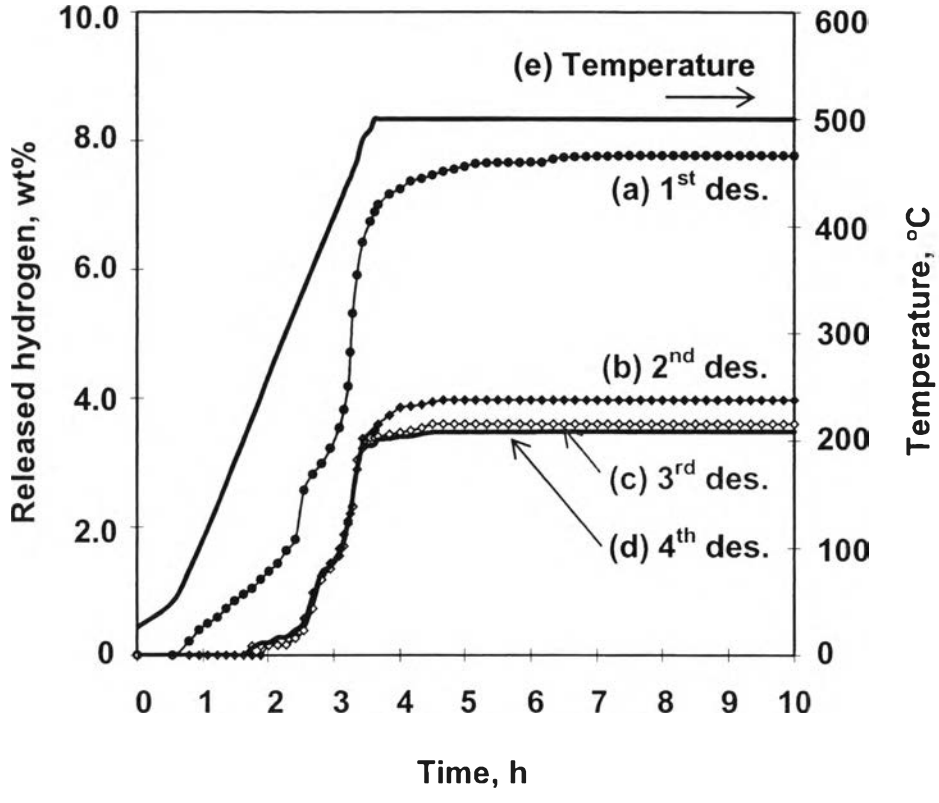

Figure 6.4 Hydrogen desorption profiles of the TiO_2-$LiBH_4$/MgH_2 mixture after ball-milling for 5 h (a) first, (b) second, (c) third, (d) forth hydrogen desorption, and (e) temperature.

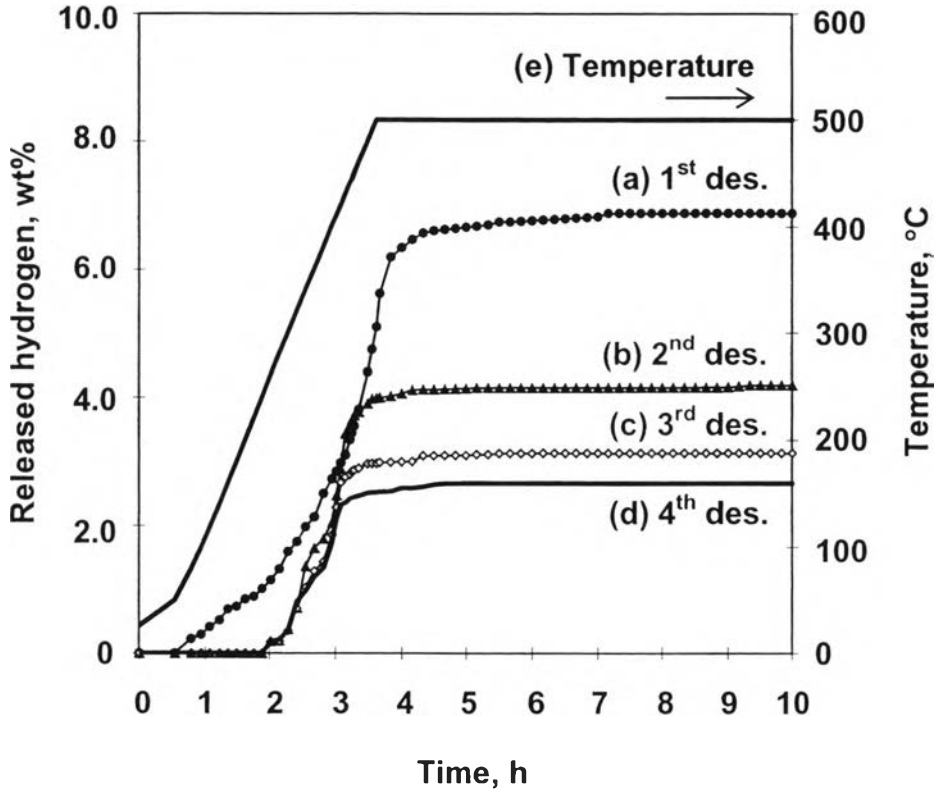

Figure 6.5 Hydrogen desorption profiles of the $TiCl_3$-$LiBH_4/MgH_2$ mixture after ball-milling for 5 h (a) first, (b) second, (c) third, (d) forth hydrogen desorption, and (e) temperature.

In the first desorption, the $LiBH_4/MgH_2$ (Fig. 6.2(a)), Ti- (Fig. 6.3(a)), and TiO_2-$LiBH_4/MgH_2$ mixtures (Fig. 6.4(a)) decompose in three steps, while the $TiCl_3$-$LiBH_4/MgH_2$ mixture (Fig. 6.5(a)) releases hydrogen in only one step. It can be deduced from the result that $TiCl_3$ somehow involves in the hydrogen dissociation of the hydrides. This can be substantiated by the formation of LiCl during the ball-milling process (Fig. 6.1(d)). For the Ti doped sample, even though there is an indication of the sample decomposition as evidenced by the presence of Li-Mg-B-Ti alloy (Fig. 6.1(b)), the decomposition of the sample is not affected. For the desorption temperature, all doped samples start to release hydrogen at the same temperature as the undoped sample, 50°C. For the amount of desorbed hydrogen, it was found that, with TiO_2 and $TiCl_3$, the samples release higher amounts of hydrogen than the undoped and Ti doped samples. From Table 6.2, the amounts of

desorbed hydrogen in the first step of the first desorption are 1.3 wt% for the undoped sample, 1.1 wt% for the Ti doped sample, and 1.8 wt% for the TiO_2 and $TiCl_3$ doped samples. Once again, the catalytic activity of TiO_2 and $TiCl_3$ shows similar effects on the $LiBH_4$ and MgH_2 mixture as that on $NaAlH_4$ [25]. On the contrary, in the case of Ti, the formation of the Li-Mg-B-Ti alloy phase may inhibit the activity of Ti resulting in the lower amount of hydrogen desorption. The lower catalytic activity of the metal catalyst than the oxide and chloride catalysts in the hydrogen desorption/absorption improvement of MgH_2 was also reported by Barkhordarian et al. [30].

Doping a titanium catalyst also decreases the hydrogen desorption temperature of the hydrides in the second step decomposition. The doped TiO_2 sample liberates hydrogen at 310°C, which is lower than that doped with Ti and the undoped one, 10 and 20°C, respectively. However, the cumulative amounts of desorbed hydrogen in this step of all doped samples are significantly lower than the undoped one. The Ti, TiO_2, and $TiCl_3$ doped samples desorb only 2.2, 2.8, and 2.2 wt% hydrogen, respectively, while the undoped sample releases 4.4 wt% hydrogen (Table 6.2). For the third step of the first desorption, the Ti- and TiO_2-$LiBH_4/MgH_2$ mixtures release hydrogen at the same temperature, 350°C, while the undoped sample desorbs hydrogen at 380°C (Table 6.2). It is clearly seen that the titanium catalysts play an important role in the reduction of the hydrogen desorption temperature.

For the total amount of desorbed hydrogen, as expected, the doped samples release lower amounts of hydrogen than the undoped one. From Table 6.2, the undoped, Ti, TiO_2, and $TiCl_3$ doped samples desorb 9.2, 8.3, 7.8, and 7.0 wt% hydrogen, respectively. The released hydrogen from the doped samples are approximately 90 (Ti), 83 (TiO_2), and 76% ($TiCl_3$) compared with the undoped sample. One possible reason is that there may be the formation of new phases during the hydrogen desorption, which will be explained by the XRD patterns after the hydrogen desorption.

Table 6.2 Hydrogen desorption temperature and total amount of desorbed hydrogen of the $LiBH_4/MgH_2$ mixture and the mixture doped with different titanium catalysts after ball-milling for 5 h in the first, second, third, and forth desorption

The $LiBH_4/MgH_2$ mixture	Starting desorption temperature, °C				Total hydrogen capacity, wt%			
	Undoped	Ti	TiO_2	$TiCl_3$	Undoped	Ti	TiO_2	$TiCl_3$
1st desorption								
- Step 1	50	50	50	50	1.3	1.1	1.8	1.8*
- Step 2	330	320	310	-	4.4	2.2	2.8	2.2**
- Step 3	380	350	350	-	9.2	8.3	7.8	7.0
2nd desorption								
- Step 1	360	390	330	310	1.8	1.7	1.4	1.3
- Step 2	450	470	420	400	4.5	5.3	4.0	4.2
3rd desorption								
- Step 1	360	390	330	310	1.8	1.7	1.4	1.3
- Step 2	450	470	420	400	3.6	5.1	3.6	3.1
4th desorption								
- Step 1	360	390	330	310	1.8	1.7	1.4	1.3
- Step 2	450	470	420	400	3.2	5.0	3.5	2.6

* The hydrogen capacity is evaluated at 320°C.

** The hydrogen capacity is evaluated at 350°C.

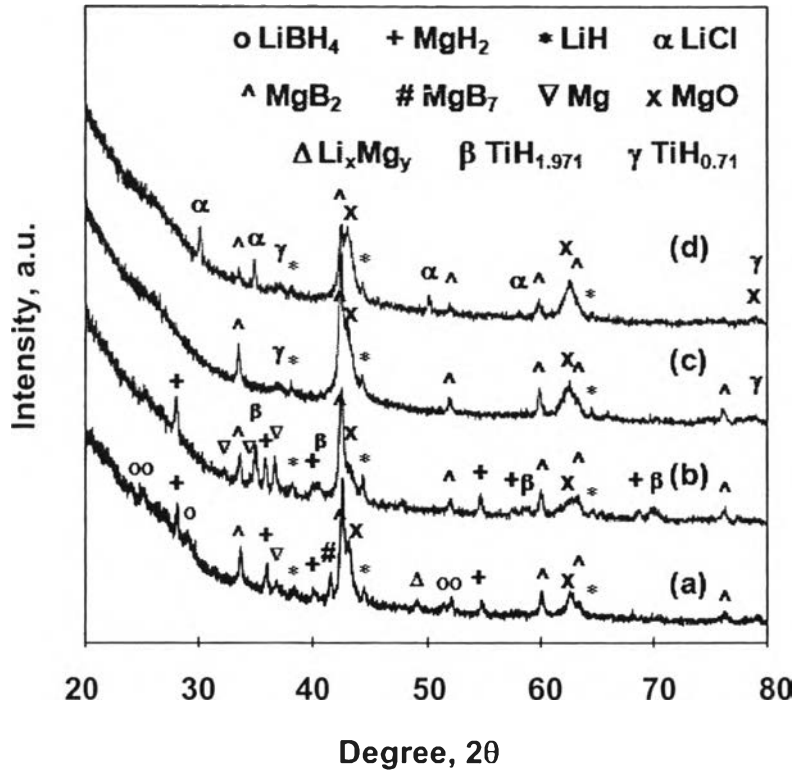

Figure 6.6 XRD patterns of the samples after the first hydrogen desorption (a) undoped, (b) Ti-, (c) TiO_2-, and (d) $TiCl_3$-$LiBH_4$/MgH_2 mixture.

The phase identification of the samples after the hydrogen desorption is shown in Fig. 6.6. It can be seen from the figure that all samples have the same phases of LiH, MgB_2, $LiBH_4$, MgH_2, and MgO. The LiH and MgB_2 phases are products from the hydrogen desorption. The presence of $LiBH_4$, MgH_2, and MgO results in the lower total amount of desorbed hydrogen than the theoretical value (11.4 wt%). $LiBH_4$ and MgH_2 are the unconverted phases of the starting materials, and MgO is the oxide layer from the reaction between Mg and impurities. This oxide layer prevents the hydrogen molecules from penetrating into the metal lattice framework. On the other hand, MgO was found to enhance the rate of hydrogen uptake [31]. In addition, the MgB_7 and Li_XMg_Y phases were found in the case of the undoped sample (Fig. 6.6(a)). The MgB_7 phase is a by-product between the reaction of rich $LiBH_4$ and MgH_2 [32], while the alloy phase of Li_XMg_Y may be from the reaction between Li and Mg [33]. The alloy phase of Li-Mg-B-Ti, which was found in the Ti doped sample after ball-milling (Fig. 1(b)), also decomposes during the

hydrogen desorption. The different titanium hydride phases were exhibited in the doped samples (Figs. 6.6(b)-(c)). The XRD patterns show that the titanium hydride phase depends on the chemical state and composition of the titanium catalyst. Doping Ti in the hydrides results in the formation of the $TiH_{1.971}$ phase, while the $TiH_{0.71}$ phase formes with TiO_2 and $TiCl_3$. A possible reason why the presence of TiO_2 and $TiCl_3$ results in the same phase of titanium hydride may be because both Ti^{4+} and Ti^{3+} defect sites in TiO_2 and $TiCl_3$, respectively, are partially reduced to the same defect site of Ti^0 during the ball-milling process [24,34-37]. Subsequently, the Ti^0 defect sites may further form a microstructure composite with the host metal lattice framework and/or transform to the titanium hydride phase of TiH_2 or $TiH_{Z<2}$ during the hydrogen desorption, Eq. (6.1) [38]. However, $TiH_{0.71}$ forms in the samples doped with TiO_2 and $TiCl_3$ instead of $TiH_{1.971}$, as detected in the one doped with Ti, because the presence of O^{2-} (in TiO_2) and Cl^- (in $TiCl_3$) may surround Ti atoms in the bulk and interfere the hydrogen uptake to form TiH_2. This phenomena also takes place for the $Ti(OBu)_4$ catalyst as proposed by Baldé et al [39]. All in all, the formation of titanium hydride, which promotes the dissociation of hydrogen molecular into hydrogen atoms [40], results in the decrease in the hydrogen desorption temperature of the $LiBH_4$ and MgH_2 mixture.

$$Ti + H_2 \rightarrow TiH_2 \quad (\Delta G_f^{\circ} = -105 \text{ kJ mol}^{-1}) \tag{6.1}$$

It is evidence that the titanium catalysts affect the total amount of desorbed hydrogen. The undoped sample has the highest total amount of hydrogen. Considering the doped samples, the one doped with Ti gives the highest total amount of desorbed hydrogen (8.3 wt%). A possible reason is due to Ti has a much lower chance to form any inactive by-products as it does not contain O^{2-} as in TiO_2 or Cl^- as in $TiCl_3$. The statement can be confirmed by the XRD patterns after the hydrogen desorption (Fig. 6.6). The patterns show that the Ti doped sample has lower MgO intensity than the other doped samples. In the case of the sample doped with TiO_2, it releases a lower amount of hydrogen than that doped with Ti. The explanation is that the oxide ions in TiO_2 may lead to the formation of inactive oxide compounds such

as B_2O_3 (ΔG_f°= -1184.1 kJ mol^{-1}) and MgO (ΔG_f°= -569.6 kJ mol^{-1}) [41]. However, only the MgO phase is observed in the XRD pattern (Fig. 6.6(c)) because the other oxide compounds may be in the amorphous form and/or present in a small quantity. The sample doped with $TiCl_3$ desorbs the lowest amount of hydrogen because it can form both MgO and LiCl phases during the hydrogen desorption (Fig. 6.6(d)).

The XRD patterns of the desorbed samples (Fig. 6.6) were used to purpose the hydrogen desorption pathway. The decomposition reaction of the undoped sample and that doped with Ti, TiO_2, and $TiCl_3$ may follow Eqs. (6.2)-(6.5).

$$2LiBH_4 + MgH_2 \rightarrow 2LiH + MgB_2 + 4H_2 \quad (6.2)$$

$$2LiBH_4 + MgH_2 + 0.09Ti \rightarrow 2LiH + MgB_2$$

$$+ 0.09TiH_{1.971} + \left(\frac{7.82}{2}\right)H_2 \quad (6.3)$$

$$2LiBH_4 + MgH_2 + 0.09TiO_2 \rightarrow 2LiH + 0.82MgB_2 + 0.18MgO$$

$$+ 0.09TiH_{0.71} + 0.36B + \left(\frac{7.94}{2}\right)H_2 \quad (6.4)$$

$$2LiBH_4 + MgH_2 + 0.09TiCl_3 \rightarrow 1.73LiH + MgB_2 + 0.27LiCl$$

$$+ 0.09TiH_{0.71} + \left(\frac{8.21}{2}\right)H_2 \quad (6.5)$$

After the first desorption, the spent hydrides were subject to the hydrogen absorption. The XRD patterns of the adsorbed samples, Fig. 6.7, show that $LiBH_4$ and MgH_2 are recovered from the reaction between LiH and MgB_2 in all samples. However, some traces of unconverted phases of LiH, Mg, MgO, $TiH_{1.971}$, and $TiH_{0.71}$ can be observed. This substantiates the incomplete hydrogen absorption of the spent sample, and that inherently affects the decrease in the total amount of desorbed hydrogen in the subsequent desorption.

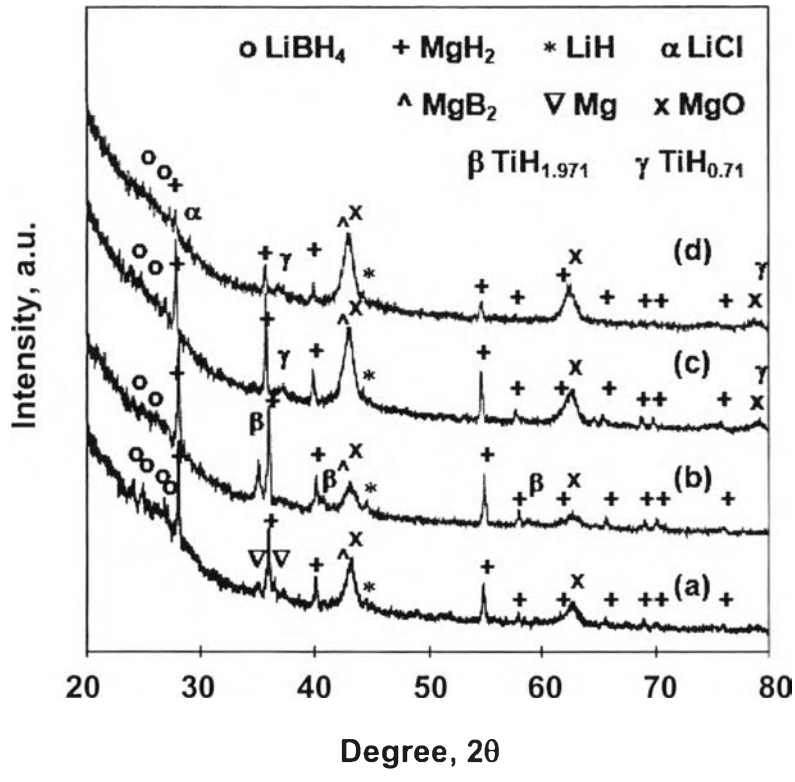

Figure 6.7 XRD patterns of the samples after the first hydrogen absorption (a) undoped, (b) Ti-, (c) TiO_2-, and (d) $TiCl_3$-$LiBH_4/MgH_2$ mixture.

For the subsequent desorption, the results from Figs. 6.2-6.5(b)-(d) exhibit that all samples decompose in two steps. The starts of the hydrogen desorption temperature in the first step are 360, 390, 330, and 310°C for the undoped sample and that doped with Ti, TiO_2, and $TiCl_3$, respectively. It was found that the TiO_2 and $TiCl_3$ doped samples release hydrogen at a lower temperature than the undoped one. On the contrary, the Ti doped sample desorbs hydrogen at a higher temperature than the undoped one. The amounts of desorbed hydrogen of the Ti, TiO_2, and $TiCl_3$ doped samples are 1.7, 1.4, and 1.3 wt%, respectively, which are lower than that of the undoped sample, 1.8 wt%. In addition, the results from Table 6.2 show that the amounts of desorbed hydrogen in the first step are constant up to the forth desorption. In the second step, the samples doped with Ti, TiO_2, and $TiCl_3$ start to release hydrogen at 470, 420, and 400°C, respectively, while the undoped sample liberates hydrogen at 440°C. It can be said that using $TiCl_3$ results in the lowest

desorption temperature, while using Ti inhibits the hydrogen decomposition of the $2LiBH_4/MgH_2$ mixture. The total amount of hydrogen in the second to the forth desorption of the samples doped with Ti, TiO_2, and $TiCl_3$ are in the range of 5.0-5.3, 3.5-4.0, and 3.6-4.2 wt% (Table 6.2), respectively, while the undoped sample releases 3.2-4.5 wt% hydrogen (Table 6.2).

6.5 Conclusions

A 2:1 molar ratio of $LiBH_4/MgH_2$ mixture was investigated with the presence of 3 mol% of a titanium catalyst for its hydrogen desorption/absorption. In the first desorption, the samples doped with $TiCl_3$ released hydrogen in one step, while the other samples decomposed in three steps. However, all samples started to desorb hydrogen at the same temperature, 50°C. The undoped sample had the highest total amount of hydrogen (9.2 wt%). In the subsequent desorption, all samples decomposed in two steps. The desorption temperatures of the samples were in the order of $TiCl_3$ > TiO_2 > undoped > Ti. However, using Ti resulted in the highest amount of reversible hydrogen at 5.0 wt%.

6.6 Acknowledgements

This work was supported by National Science and Technology Development Agency (Reverse Brain Drain Project); Royal Jubilee Ph.D. Program (Grant No. PHD/0249/2549), Thailand Research Fund; The Petroleum and Petrochemical College (PPC); Research Unit for Petrochemical and Environment Catalysis, Ratchadapisak Somphot Endowment; the Center of Excellence on Petrochemical and Materials Technology, Thailand; and UOP, A Honeywell Company, USA.

6.7 References

[1] Satyapal S, Petrovic J, Read C, Thomas G, Ordaz G. The U.S. department of energy's national hydrogen storage project: progress towards meeting hydrogen-powered vehicle requirements. Catalysis Today 2007;120:246-256.

[2] Schlapbach L, Züttel A. Hydrogen-storage materials for mobile applications. Nature 2001;414:353-358.

[3] Züttel A, Borgschulte A, Orimo S-I. Tetrahydroborates as new hydrogen storage materials. Scripta Materialia 2007;56:10:823-828.

[4] Principi G, Agresti F, Maddalena A, Russo SL. The problem of solid state hydrogen storage. Energy 2009;34:12:2087-2091.

[5] Bogdanović B, Schwickardi M. Ti-doped alkali metal aluminium hydrides as potential novel reversible hydrogen storage materials. Journal of Alloys and Compounds 1997;253-254:1-9.

[6] Sandrock G, Gross K, Thomas G. Effect of Ti-catalyst content on the reversible hydrogen storage properties of the sodium alanates. Journal of Alloys and Compounds 2002;339:1-2:299-308.

[7] Blanchard D, Brinks HW, Hauback BC, Norby P. Desorption of LiAlH4 with Ti- and V-based additives, Materials Science and Engineering 2004;108:54-59.

[8] Liang G, Huot J, Boily S, Van Neste A, Schulz R. Hydrogen storage properties of the mechanically milled MgH_2-V nanocomposite. Journal of Alloys and Compounds (1999) 291;1-2: 295-299.

[9] Hanada N, Ichikawa T, Hino S, Fujii H. Remarkable improvement of hydrogen sorption kinetics in magnesium catalyzed with Nb_2O_5. Journal of Alloys and Compounds (2006) 420;1-2:46-49.

[10] Fedneva EM, Alpatova VL, Mikheeva VI., Russian Journal of Inorganic Chemistry 1964;9:6:826–827.

[11] Liang G, Huot J, Boily S, van Neste A, Schulz R. Catalytic effect of transition metals on hydrogen sorption in nanocrystalline ball milled MgH_2–T_m (T_m = Ti, V, Mn, Fe and Ni) systems. Journal of Alloys and Compounds 1999;292:247-252.

[12] Shulz R, Huot J, Liang G, Boily S, Lalande G, Denis MC. Recent developments in the applications of nanocrystalline materials to hydrogen technologies. Materials Science Engineering: A 1999;267:240-245.

[13] Kang X-D, Wang P, Ma L-P, Cheng H-M. Reversible hydrogen storage in $LiBH_4$ destabilized by milling with Al. Applied Physics A: Materials Science & Processing 2007;89(4):963-966

[14] Züttel A, Rentscha S, Fischerb P, Wengera P, Sudana P, Maurona Ph, Emmenegger Ch. Hydrogen storage properties of $LiBH_4$. Journal of Alloys and Compounds 2003;356-357:515-520.

[15] Züttel A, Wenger P, Rentsch S, Sudan P, Mauron Ph, Emmenegger Ch. $LiBH_4$ a new hydrogen storage material. Journal of Power Sources 2003;118:1-2:1-7.

[16] Au M, Jurgensen A. Modified lithium borohydrides for reversible hydrogen storage. Journal of Physical Chemistry B 2006;110:13:7062-7067.

[17] Au M, Jurgensen A, Zeigler K. Modified lithium borohydrides for reversible hydrogen storage (2). Journal of Physical Chemistry B 2006;110:51:26482-26487.

[18] Au M, Jurgensen A, Spencer WA, Anton DL, Pinkerton FE, Hwang S-J, Kim C, Bowman RC, Jr. Stability and reversibility of lithium borohydrides doped by metal halides and hydrides. Journal of Physical Chemistry C 2008;112:47:18661-18671.

[19] Vajo JJ, Olson GL. Hydrogen storage in destabilized chemical systems. Scripta Materialia 2007;56:10:829-834.

[20] Barkhordarian G, Klassen T, Dornheim M, Bormann R. Unexpected kinetic effect of MgB_2 in reactive hydride composites containing complex borohydrides. Journal of Alloys and Compounds 2007;440:L18-L21.

[21] Barkhordarian G, Klassen T, Bormann R. Patent pending, German Pub. No: DE102004/061286, 2004.

[22] Vajo JJ, Skeith SL. Reversible storage of hydrogen in destabilized $LiBH_4$. Journal of Physical Chemistry B 2005;109:9:3719-3722.

[23] Fan M-Q, Sun L-X, Zhang Y, Xu F, Zhang J, Chu H-L. The catalytic effect of additive Nb_2O_5 on the reversible hydrogen storage performances of $LiBH_4$-MgH_2 composite. International Journal of Hydrogen Energy 2008;33:74-80.

[24] Chen J, Kuriyama N, Xu Q, Takeshita HT, Sakai T. Reversible hydrogen storage via titanium-catalyzed $LiAlH_4$ and Li_3AlH_6. Journal of Physical Chemistry B 2001;105:11214-11220.

[25] Suttisawat Y, Rangsunvigit P, Kitiyanan B, Kulprathipanja S. A reality check on using $NaAlH_4$ as a hydrogen storage material. Journal of Solid State Electrochemistry 2010;14:1813-1819.

[26] Kim J-H, Shim J-H, Cho YW. On the reversibility of hydrogen storage in Ti- and Nb-catalyzed $Ca(BH_4)_2$. Journal of Power Sources 2008;181:140-143.

[27] Hanada N, Ichikawa T, Fujii H. Catalytic effect of nanoparticle 3d-transition metals on hydrogen storage properties in magnesium hydride MgH_2 prepared by mechanical milling. Journal of Physical Chemistry B 2005;109:15:7188-7194.

[28] Yang J, Sudik A, Wolverton C. Destabilizing $LiBH_4$ with a metal (M = Mg, Al, Ti, V, Cr, or Sc) or metal hydride (MH_2 = MgH_2, TiH_2, or CaH_2). Journal of Physical Chemistry C 2007;111:51: 19134-19140.

[29] Fátay D, Révész Ă, Spassov T. Particle size and catalytic effect on the dehydriding of MgH_2. Journal of Alloys and Compounds 2005;399: 237-241.

[30] Barkhordarian G, Klassen T, Bormann R. Fast hydrogen sorption kinetics of nanocrystalline Mg using Nb_2O_5 as catalyst. Scripta Materialia 2003;49(3):242-246.

[31] Hjort P, Krozer A, Kasemo B. Hydrogen sorption kinetics in partly oxidized Mg films. Journal of Alloys and Compounds 1996;237:74-80.

[32] Alapati SV, Johnson JK, Sholl DS. Identification of destabilized metal hydrides for hydrogen storage using first principles calculations. Journal of Physical Chemistry B 2006;110:8769-8776.

[33] Yu XB, Grant DM, Walker GS. A new dehydrogenation mechanism for reversible multicomponent borohydride systems - the role of Li-Mg alloys. Chemical Communications 2006;37:3906-3908.

[34] Bogdanović B, Brand RA, Marjanovic A, Schwickardi M, Tölle J. Metal-doped sodium aluminium hydrides as potential new hydrogen storage. Journal of Alloys and Compounds 2000;302:36-58.

[35] Schüth F, Bogdanović B, Felderhoff M. Light metal hydrides and complex hydrides for hydrogen storage. Chemical Communications 2004; 2249-2258.

[36] Léon A, Kircher O, Rothe J, Fichtner M. Chemical state and local structure around titanium atoms in $NaAlH_4$ doped with $TiCl_3$ using X-ray absorption spectroscopy. Journal of Physical Chemistry B 2004;108: 16372-16376.

[37] Léon A, Schild D, Fichtner M. Chemical state of Ti in sodium alanate doped with $TiCl_3$ using X-ray photoelectron spectroscopy. Journal of Alloys and Compounds 2005;404-406: 766-770.

[38] Barin I. Thermochemical data of pure substances. 3rd edition. Weinheim: Wiley-VCH; 1995. p. 1006.

[39] Baldé CP, van der Eerden A MJ, Stil HA, de Groot F MF, de Jong KP, Bitter JH. On the local structure of Ti during in situ desorption of $Ti(OBu)_4$ and $TiCl_3$ doped $NaAlH_4$. Journal of Alloys and Compounds 2007;446-447:232-236.

[40] Xiao X, Chen L, Wang X, Wang Q, Chen C. The hydrogen storage properties and microstructure of Ti-doped sodium aluminum hydride prepared by ball-milling. International Journal of Hydrogen Energy 2007;32: 2475-2479.

[41] http://www.scribd.com/doc/50677099/Delta-G-Formacion.